

***PROCEEDINGS***  
**TWENTIETH WORKSHOP**  
**GEOTHERMAL RESERVOIR ENGINEERING**

**January 24-26, 1995**



**Stanford Geothermal Program  
Workshop Report SGP-TR-150**

## **DISCLAIMER**

**This report was prepared as an account of work sponsored by an agency of the United States Government. Neither the United States Government nor any agency Thereof, nor any of their employees, makes any warranty, express or implied, or assumes any legal liability or responsibility for the accuracy, completeness, or usefulness of any information, apparatus, product, or process disclosed, or represents that its use would not infringe privately owned rights. Reference herein to any specific commercial product, process, or service by trade name, trademark, manufacturer, or otherwise does not necessarily constitute or imply its endorsement, recommendation, or favoring by the United States Government or any agency thereof. The views and opinions of authors expressed herein do not necessarily state or reflect those of the United States Government or any agency thereof.**

## **DISCLAIMER**

**Portions of this document may be illegible in electronic image products. Images are produced from the best available original document.**

## HDR RESERVOIR ANALYSIS INCORPORATING ACOUSTIC EMISSION DATA

J. Willis-Richards<sup>1</sup>, K. Watanabe<sup>2</sup>, T. Yamaguchi<sup>3</sup>, Y Sato<sup>4</sup> and S. Takasugi<sup>5</sup>

1 Dept. of Resources Engineering, Tohoku University, Sendai 980, Japan

2 Research Institute for Fracture Technology, Tohoku University, Sendai 980, JAPAN

3 National Institute for Resources and Environment, 16-3 Onogawa, Tsukuba-shi, Ibaraki, 305, JAPAN

4 NEDO, Geothermal Energy Dept., Sunshine 60, Higashi-Ikebukuro 3-1-1, Toshima, Tokyo 170, Japan

5 Geothermal Energy Research and Development Co., Ltd., Kyodo Bldg., 11-7 Kabuto-cho, Nihonbashi, Chuo-ku, Tokyo 103, Japan

### ABSTRACT

A set of models of HDR systems is presented which attempts to explain the formation and operation of HDR systems using only the in-situ properties of the fractured rock mass, the earth stress field, the engineering intervention applied by way of stimulation and the relative positions and pressures of the well(s).

A statistical and rock mechanics description of fractures in low permeability rocks provides the basis for modeling of stimulation, circulation and water loss in HDR systems. The model uses a large number of parameters, chiefly simple directly measurable quantities, describing the rock mass and fracture system.

The effect of stimulation (raised fluid pressure allowing slip) on fracture apertures is calculated, and the volume of rock affected per volume of fluid pumped estimated. The total rock volume affected by stimulation is equated with the rock volume containing the associated AE (microseismicity). The aperture and compliance properties of the stimulated fractures are used to estimate impedance and flow within the reservoir. Fluid loss from the boundary of the stimulated volume is treated using radial leak-off with pressure-dependent permeability.

The model is applied to HDR stimulation and circulation experiments carried out at Rosemanowes, UK (1983-1989) and at Hijiori, Japan (1986-1991).

### INTRODUCTION

The linked models of stimulation, circulation and water loss presented here use simple rock mechanics applied to a population of (circular) fractures in an attempt to reach an understanding of the creation and operation of HDR systems. Worldwide HDR experiments and other field observations over the past 15 years (CSM Associates, 1992) suggest:

- The rock mass is subject to anisotropic, remotely generated lithospheric stresses
- Fracture lengths can often be described by fractal distributions
- The in situ permeability of the natural fracture systems in crystalline basements selected for HDR experiments is generally  $1 - 100 \mu\text{D}$  (e.g. Clauser, 1992). Circulation through such systems, unmodified, would have unacceptably high impedance and water losses
- High pressure fluid injection, by reducing the normal stress on fractures, enables slip to take place. In strong rocks slipping at low normal stress this generally leads to a significant increase in fracture aperture and permeability. A small fraction of the slip is unstable and causes AE, which may be located, typically appearing as structured ellipsoidal clouds
- The ratio of the permeability within the stimulated volume (AE cloud) to that outside it is high, generally several orders of magnitude
- It appears to be difficult to create extensive new fractures in anisotropically stressed and pre-fractured crystalline rock
- The position of recovery wells in relation to the injection well, fracture orientations and the earth stresses exerts a strong effect on production. Optimal positioning has yet to be determined
- Steady state water losses increase more than linearly with reservoir mean pressure

These considerations suggest that "first principles" models should contain the following elements:

- Description of fracture lengths, orientations, compliance and shear behavior; the rock elastic properties; the in-situ fluid pressure and stresses.
- A treatment of stimulation which describes the resulting fracture aperture distribution and makes predictions that can be verified against AE locations
- A treatment of circulation which uses the stimulated fracture properties and their geometry in relation to the wells, the earth stresses and the pressure distribution

- A treatment of water loss from the margins of the stimulated region

For HDR application, the complexity of explicit 3-D geometric fracture representations and the computational demands of coupled flow solvers are disproportionate to our knowledge of the actual geometry of the fracture system, which, in any case, we believe to be "well connected".

The objectives of the models presented here are to predict field production, impedance and water loss data from experimental or hypothetical HDR systems with the minimum of model calibration involving input parameters that can not be measured, at least in principle, in the field or laboratory.

#### ROCK MASS DESCRIPTION

Fracture orientation data is gathered from borehole wall images or core. For each visible fracture, the orientation and length of observed fracture should be recorded. Fracture orientation can be simulated by resampling the observed data set, using the length of fracture observed as a "weight" thereby removing any geometric observational censoring of the fracture network without recourse to analytic corrections. The fracture density, at the resolved fracture length scale, can be estimated directly as the total recovered fracture area divided by the core volume.

Fracture lengths, at the scale of interest for HDR circulation (> about 2m), are typically unmeasurable for HDR reservoirs. This is potentially a very serious problem, since the proportion of longer fractures determines the ease with which large shear displacements, and hence large apertures, may be created. Main et al. (1990) state that much of the current observation of trace lengths in outcrop for quasi-stable fracture systems suggest that the length distributions are characteristically fractal, with fractal dimension ( $D_L$ ) close to 1.0.

A first order approximate simulation of a fracture network can, therefore, be made knowing only the fracture orientation distribution and the fracture density (e.g. Watanabe and Takahashi, 1995). Whilst the models used here do not simulate the fracture network explicitly, they make use of both the fracture density and the fracture length distribution. A default value for  $D_L$  of 2.0 for fracture radii (equivalent to an  $D_L$  of 1.0 for outcrop trace length distribution) is used.

Fracture in-situ apertures, closure and shear behavior can be obtained from laboratory experiment carried out on core specimens or on samples of outcropping analog fractures. Their effects on stimulation and circulation, as expressed through the model, are not dependent on the fine detail of the chosen constitutive laws, but a clear distinction can be drawn between weak or strong asperities, and rough or smooth fractures.

Water loss from an HDR system is dependent on the far

field in-situ permeability, usually at hydrostatic pressures. There also appears to be a scale effect, with higher permeability observed at increasingly larger scales up to about 100m. Permeability should be measured from low pressure injections into long open hole lengths and with large radii of investigation (both  $> 100m$ ). Even when careful measurements are made, considerable uncertainty, perhaps up to nearly an order of magnitude, may still remain. In as much as the in situ permeability is uncertain, so are predictions of water loss.

Rock elastic properties may be measured from core specimens or from logs.

Calculation of the response of the fractures to fluid injection requires knowledge of the in situ stresses. One principal axis of the stress tensor is assumed to be normal to the earth's surface, and its magnitude given by the weight of overburden (but see Cornet and Burlet, 1992). The orientation of the remaining axes may be determined from borehole breakouts, drilling induced fracture orientation, differential strain curve analysis (i.e. microcrack orientation) or hydraulic fracturing. Where stress directions are coherent over wide areas, a good estimate of the maximum principal stress direction can be found in the world stress map (Zoback, 1992).

The stress magnitudes are also needed. If direct estimates of the magnitude of  $\sigma_{min}$  (usually one of the horizontal stresses in deep HDR sites) from hydraulic fracturing or ISIP analysis are not available then indirect indicators should be used. These may include the pressure at which AE are first induced, or analysis of microseismic focal mechanisms.

#### STIMULATION MODEL

HDR stimulation is the creation of irreversible increases in fracture aperture by high pressure fluid injection through shear movement of rough fracture surfaces in stressed rock. Since the apertures produced during stimulation are high (of order 1 mm), the stimulation volume is considered to be at a single uniform pressure and bounded by a narrow region in which much active shear is taking place and across which pressures drop rapidly to hydrostatic. The effects of stimulation on an individual fracture can be calculated by:

1. Assessing frictional stability using a simple Coulomb friction law
2. Noting that shear stiffness is proportional to the fracture radius and so calculating the amount of slip
3. Calculating the increase in aperture that results

By noting the increase in aperture of many fractures and knowing the fracture density, the ratio of the volume of fluid injected to the volume of rock affected can be calculated. This is termed the **rock / fluid ratio** (RFR), see Willis-Richards (1995) for details of the calculations involved.

An estimate of the RFR is necessary to correctly calculate

the "backstress" terms. Any one of a number of analytical solutions available for the stresses imposed by the expansion of a flattish ellipsoid in an elastic medium (e.g. Eshelby, 1957) may be used.

The stimulation model produces a collection of stimulated fractures, each defined by its orientation, length, and shear displacement. The RFR estimate can be compared with the volume of the microseismic cloud generated divided by the volume of fluid injected. Typical RFR ratios can vary from about 2000:1 for high pressure injection into rough fractures with high stress anisotropy ( $\sigma_1 - \sigma_3$ ) and hence high potential for fracture opening by shear dilation, to 30,000:1 or more for lower pressure injections that are just able to cause widespread shear movement.

Stimulation design objectives are to minimize the pressure used and hence the fluid volume required, whilst at the same time ensuring that the reservoir created has low enough impedance. Low impedance ensures a low mean reservoir operating pressure and hence minimizes far field fluid losses, as well as reducing parasitic pumping requirements. Excessive pressure during stimulation increases costs through the higher fluid volume requirement and possibly through the need to use gel rather than water. Too much fluid pumped leads to too large a stimulated volume, which results in high far field losses.

The critical operationally controllable parameter for HDR stimulation, therefore, is the pressure. Changes in flow rate will have little effect on resulting apertures unless the change in treatment pressure is significant, but may expand the stimulated volume until the injection rate balances far field losses.

In the case of a seismogenic circulation, which is a "progressive stimulation", the critical pressure is a mean reservoir pressure, approximately determined as a weighted average of injection and recovery well pressures.

## CIRCULATION MODEL

The stimulated fractures are the main resource from which a picture of the circulation is drawn. Since we seek to avoid a complex 3-D simulation of the fracture network, simple geometric combinations of fractures which reflect flow paths across the reservoir are sought. A single such flow path can be envisaged as the series of fractures traced by fluid crossing the reservoir.

A large number of flow paths are simulated, and the fracture area and impedance of each calculated. The total fracture area to simulate, the total flow and the resulting flow-area distribution can be assessed by comparison with suitably analyzed field data from a well studied reservoir, such as the Rosemanowes Phase 2B system. Agreement validates the flow path generation method, at least for the particular reservoir used for calibration.

The model assumes that if the flow-area distribution for

the Rosemanowes Phase 2B reservoir, deduced from tracer and thermal draw down data by Nicol and Robinson (1990), Table 1, can be matched by the flow path generator chosen, then useful results can be obtained for other sites when the total fracture area is suitably scaled by the well separation. Naturally, other fracture orientations, stresses and well geometries will automatically generate other flow-area distributions; but these should be appropriate for the sites in question if the flow path generator chosen is sensible.

Table 1: Reservoir flow / area distribution determined by Nicol and Robinson (1990) for the Rosemanowes RH12 - RH15 Phase 2B reservoir as 4 flow paths

Flow path area (m <sup>2</sup> )	Flow %	Cumulative area %	Cumulative flow %
7400	15.1	2.6	15.1
40400	34.2	16.6	49.3
130300	39.6	61.7	88.9
110500	11.1	100.0	100.0

It turns out (fortuitously?) that the simplest possible flow path geometry, that of overlapping fractures in series, figure 1, can generate suitable flow-area distributions.

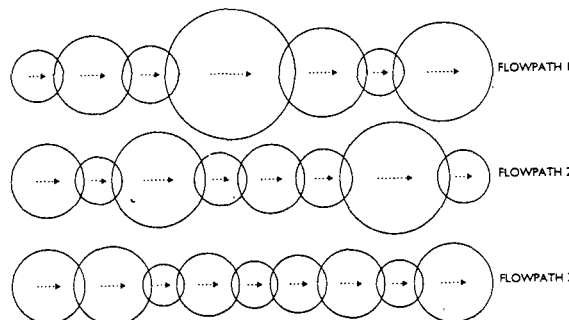


Fig. 1. Conceptual model of reservoir made up of a number of linear flow paths

Two parameters, fracture path tortuosity ( $T_{path}$ ) and the ratio of total simulated fracture area to reservoir flowing fracture area, are available for customizing the fit to the Rosemanowes Phase 2B data. A good fit is achieved with  $T_{path} \approx 1.3$  and fracture area ratio 2.5, figure 2. The fit obtained to the experimental cumulative area / cumulative flow curve for the Rosemanowes reservoir means that the flow model should similarly be able to reproduce the tracer and thermal draw down results, were these aspects to be included.

The model can be simply, but approximately, adapted to multiple well configurations, provided that each set of flow paths is treated independently i.e. there is no flow interference between paths.

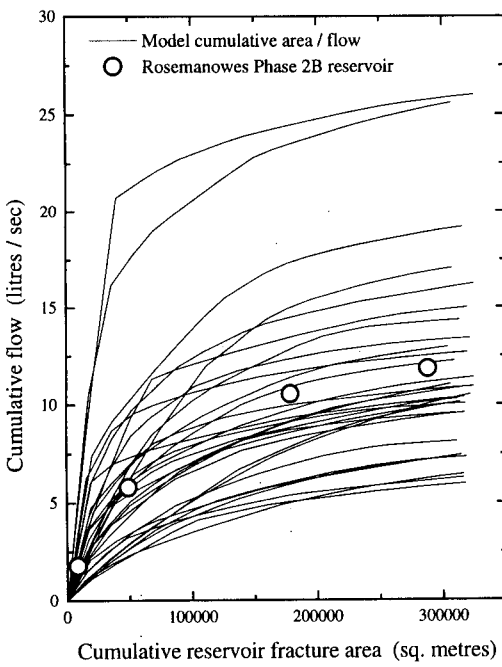


Fig. 2 30 realizations of the flow model for the Phase 2B circulation. Flow paths sorted in order of flow density and plotted as cumulative flow against cumulative fracture area. Field data from Nicol and Robinson (1991).

Results quoted below are the mean of 100 realizations of the flow paths concerned. The variance of individual well production flow is, as might be expected, quite high, but the relative magnitudes of production from the different wells are generally preserved.

#### WATER LOSS MODEL

Circulation takes place towards the center of a stimulated volume of high permeability. Fluid loss, on the other hand, is leak off from the margins of this volume and is controlled by the in-situ permeability and its response to fluid pressure change in the sub-seismogenic pressure range. Fluid losses are not a function of the injection or recovery flow rates as such, but rather of the mean reservoir pressure seen at the margin of the stimulated volume and of its surface area. The injection and recovery pressures, weighted by their flow rates, are used to estimate the mean reservoir pressure, somewhat after the manner of Brown (1994).

At sub-seismogenic fluid pressures, permeability changes will be most strongly controlled by the response to changes in effective stress of the most compliant fractures. Such fractures are those sub-parallel to the maximum principal stress i.e. with the minimum normal stresses. Typical fracture compliance curves can be measured or otherwise estimated from generic data. The cube of the ratio of fracture apertures at some fluid pressure  $P$  and at the in-situ fluid pressure can thus be used to calculate the

change in permeability with pressure (the "cubic" flow law implicitly assumed).

An aperture compliance law, together with the measured in situ permeability and an equivalent radius for the stimulated volume, lets us calculate the water loss for a given pressure drop by numerical integration from the edge of the stimulated region outwards. This simple model, which has a reasonable physical and geometric basis, gives the commonly observed super-linear relationship between mean reservoir pressure and water loss.

Extra fluid losses can also take place during "steady state" circulation if AE events are being produced. The process is identical with that during stimulation. A significant fraction of the high water losses experienced during seismogenic circulation at various sites can be ascribed to this mechanism. Quantitative examination of the importance of this mechanism is possible using the stimulation and water loss models together. The great expansion of the stimulated volume accompanying circulation AE will result in a permanent increase in the water loss rate from the reservoir, even when the mean reservoir pressure is reduced to sub-seismogenic levels.

The water loss model is incorporated within the circulation model, but may be used in isolation if required.

#### APPLICATION TO PHASE 2A AND 2B CIRCULATION EXPERIMENTS, ROSEMANOWES, CORNWALL, UK

The Phase 2B (1985-1989) circulation from well RH12 to well RH15 over a distance of 190m took place within a small volume of rock ( $\sim 10^7 \text{ m}^3$ ), stimulated by a viscous fluid injection ( $\sim 12-14 \text{ MPa}, 5500 \text{ m}^3$ ) in 1985 (Richards et al., 1994). However, this reservoir was contained within a much larger ( $\sim 6 \times 10^8 \text{ m}^3$ ) stimulated volume created during Phase 2A (1983) by a prolonged seismogenic circulation between wells RH12 and RH11 at injection pressures of about 8 - 12 MPa. A total of about  $10^5 \text{ m}^3$  of water was lost creating this microseismic cloud, a water to rock ratio of about 6000:1 without correction for aseismic leakoff to the far field.

Fracture orientations are simulated by resampling the BHTV database, a fracture  $D_L$  of 1 is assumed. Stresses were measured by hydraulic fracturing and a number of other methods (Pine et. al, 1990)

#### Phase 2A

For the Phase 2A "seismogenic circulation" a mean reservoir pressure in the range 6 to 10 MPa is investigated. Table 2 shows the range of RFR to be expected for these injection pressures and the water losses from the margins of the seismic cloud, using a far field permeability of  $20 \mu \text{D}$ . A self consistent picture of fluid loss and stimulation emerges for a mean reservoir pressure of about 8 MPa, consistent with typical recoveries of about 30 - 40% at the higher injection pressures.

Table 2: Phase 2A "circulation - stimulation" water budget and rock/fluid ratios (RFR)

Average reservoir pressure MPa	Maximum fluid loss rate l/sec	Estimated total fluid loss m <sup>3</sup>	RFR observed adjusted for fluid loss	RFR calculated
6	5.6	22000	7700	19000
7	7.5	29000	8500	13000
8	10.0	39000	9800	9200
9	13.3	52000	12500	6800

The Phase 2A circulation took place within a more restricted rock volume created by the RT2A046 - RT2A051 stimulations at pressures of about 11 - 12 MPa. Using this stimulation pressure to create a file of stimulated joints as input, the circulation model suggests appropriate flow rates and recoveries of about 75% for RH12 - RH11 circulation, provided that the circulation was aseismic. This is consistent with the relatively high recovery rates for the low injection pressure circulations during Phase 2A. The high Phase 2A water losses appear to be due to the continuous AE expansion of the stimulated volume, creating void space by shear dilation, combined with increased potential for marginal water loss as the stimulated volume expanded. A much improved Phase 2A reservoir could have been created by proppant placement around the recovery well, reducing the mean reservoir pressure to sub-seismogenic values at acceptable injection rates.

#### Phase 2B

The RT2B022 viscous gel stimulation determined the inter well fracture apertures for the Phase 2B circulation. Well head pressures of 14.4 MPa suggest formation treatment pressures of about 12 MPa. This stimulation took place from RH15, ensuring that the highest pressures were seen by the fractures near the production well. The observed RFR inferred from AE locations, was about 2000:1. The actual RFR was likely to have been somewhat greater due to leadoff into the Phase 2A stimulated volume. For a 12 MPa stimulation the predicted RFR is 3400:1.

Using this stimulation pressure to describe the circulation fracture apertures, the predicted injection and fluid loss rates are shown in Figure 3, together with field data from Phase 2B. The simulated flow area was 288,000m<sup>2</sup>, as calculated by Nicol and Robinson. As was the case in Phase 2A, the actual injection rates and water loss increase markedly when AE start, at mean reservoir pressures of about 6 MPa. The improved production well treatment and more favorable production flow path direction, reduced the impedance and thereby lowered the mean reservoir pressure for a given injection flow rate. The improved recovery and impedance thus allowed high

recoveries to persist to higher injection pressures and much higher injection flow rates.

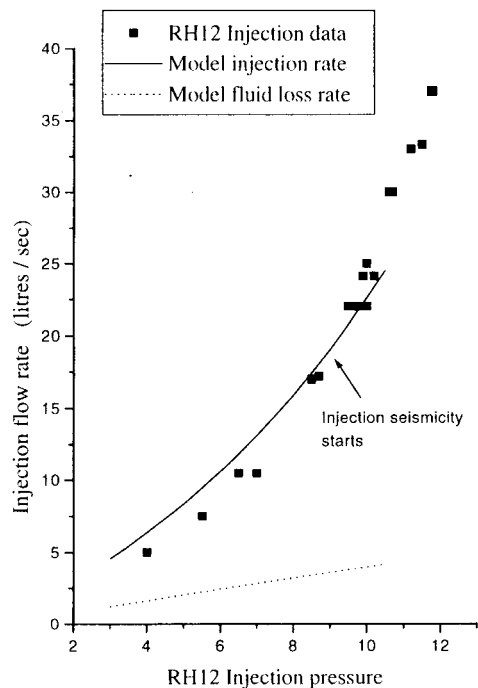


Fig 3. Model injectivity, water loss and actual injectivity data for the RH12-15 Phase 2B (1985-1989) circulation at Rosemanowes.

These quantitative estimations of rock mass response and fluid flow at Rosemanowes are only possible given suitable values of the "unmeasurable" input parameters (total simulated flow path area, mean flow path tortuosity). The values used, however, are reasonable and are carried forward for use with the Hijiori reservoir below.

The concepts within the model allow a synthesis of stimulation, fluid loss, seismicity and circulation for the Phase 2A and 2B experiments at Rosemanowes that has hitherto been lacking.

#### APPLICATION TO THE HIJIORI HDR PROJECT, YAMAGATA PREFECTURE, JAPAN

HDR experiments have taken place at Hijiori in a shallow (1800m) reservoir since 1985 (Matsunaga et al., 1990; NEDO, 1987-1992; CSM Associates, 1992). Stimulation was from the injection well (SKG-2) and recovery from up to three wells (HDR-1, HDR-2 and HDR-3) which were progressively added to the system. Experimentation on this "shallow" reservoir culminated in 1991 with a three month circulation test using all three production wells.

Fracture orientations for modeling were simulated by resampling 229 measurements made on core from well HDR-3, figure 4.

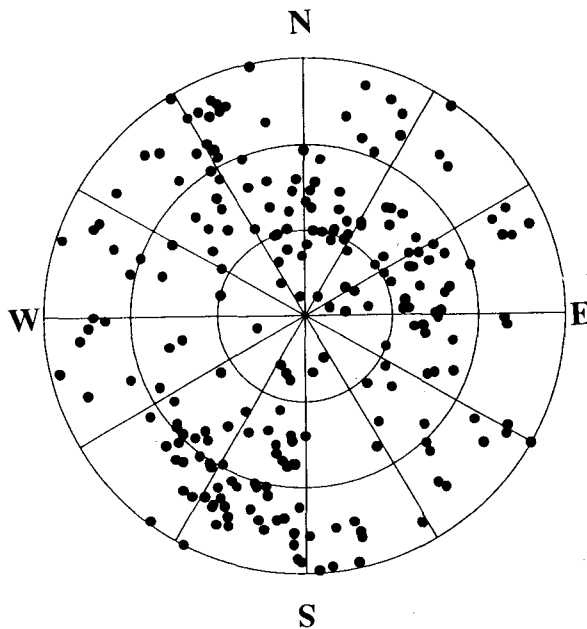


Fig. 4. Polar plot of normals to fractures measured in oriented core recovered from well HDR-3.

The stress data are somewhat ambiguous, but information includes DSCA measurements on core, ISIP and pressure / flow histories, AE focal mechanisms and observation of the minimum fluid injection pressure required to cause AE. The far field permeability has not been determined at low injection pressures, but appears to be higher than that at Rosemanowes; the modeling reported here uses a value of  $60\mu\text{D}$ .

The history of experimentation can be divided into 4 parts:

1. Early stimulations 1985 - 1988
2. Exp. 8505 seismogenic circulation
3. Exp. 8902 seismogenic circulation
4. Exp. 9102 aseismic circulation

#### *Early stimulations*

A total of about  $3500\text{m}^3$  of water was injected into SKG-2 at well head pressures of up to about 15 MPa. Allowing for depressurizations and reinflations, the effective pumped volume was probably about  $2500\text{m}^3$ , and estimated friction losses suggest formation treatment at about 13 MPa for which an RFR of 2600:1 is calculated. The volume of the AE cloud created was about  $9 \times 10^6 \text{ m}^3$  (NEDO, 1988, p20) giving an observed RFR of about 3600:1. Fluid loss estimates, based on the compliant fracture model described above, suggest aseismic leakoff during the stimulation of 10 - 20 liters /sec, about 15 - 30% of the mean fluid injection rate and consistent with the two estimates of the RFR. The fracture properties determined by these stimulations are used to calculate subsequent circulation performance.

#### *Exp. 8502 seismogenic circulation*

$13600\text{m}^3$  of water was injected into SKG-2 over 14 days at a rate of 16.7 l/sec and well head pressures of 5.5 to 6.1 MPa. About 35% was recovered from HDR-1. 70 AE were located, defining a cloud of about  $60 \times 10^6 \text{ m}^3$ .

The stimulation and water loss models suggest an RFR of about 25000:1 and water losses of up to 16 l/sec when the AE cloud is fully developed. It appears likely that the majority of the actual water loss took place aseismically at the margins of the growing AE cloud, and that only about  $2000\text{m}^3$  of the  $10000\text{m}^3$  total water loss was due to shear dilation.

The circulation model, when applied within this extended AE cloud and using a total reservoir fracture area of  $10000\text{m}^2$ , suggests recovery of about 30% from HDR-1 with total injection of about 15 l/sec, both very close to the actual figures.

#### *Exp. 8805 seismogenic circulation*

$46000\text{m}^3$  of water were injected into SKG-2 over 29 days at a rate of 18 l/sec and well head pressures of 4.5 to 5.0 MPa. Over 400 AE events were recorded, defining a cloud of about  $250 \times 10^6 \text{ m}^3$  (NEDO, 1989, p55). Despite both HDR-1 and HDR-2 being allowed to flow, total recovery was still only about 34%, about 8% from HDR-1 and 26% from HDR-2 (NEDO, 1991, p13).

The stimulation and water loss models suggest an RFR of 65000:1 and water losses of up to about 12 l/sec when the AE cloud is fully developed. Thus, of the  $26000\text{m}^3$  of water loss, about  $3000 - 4000 \text{ m}^3$  was due to shear dilation, the remainder, about 9 l/sec leaking off into the formation aseismically.

The circulation model, adapted to two wells with a total reservoir fracture area of  $25000\text{m}^2$  contained within the newly extended AE volume, predicts about 45 - 50% total recovery split, in the ratio 1:4 between HDR-1 and HDR-2. Total injection flow is about 20% overestimated. The higher production from HDR-2 is due to a better alignment with respect to SKG-2 and the joint and stress orientations (achieved through using the AE cloud as a drilling target) which allows more direct communication via large aperture fractures.

The failure to improve recovery was due to the expansion of the AE cloud, water losses being caused by both active shear dilation and the increase in surface area.

#### *Exp. 9102 aseismic circulation*

$90000\text{m}^3$  of water was injected over 3 months at about 18 l/sec and well head pressures of 3.0 to 4.0 MPa. No AE were detected. A total recovery of about 75% was obtained, distributed in the ratio of about 1:2:2 between HDR-1, HDR-2 and HDR-3 respectively.

The water loss model, applied within the  $250 \times 10^6 \text{ m}^3$  AE cloud created by Exp. 8902, gives a water loss rate of 5.5 l/sec using the weighted mean reservoir pressure, close to the actual loss rate of just over 4 l/sec. The circulation

model gives predicted recovery rates in the ratio 2:10:7 from HDR-1, HDR-2 and HDR-3 with total recovery of about 70%, figure 5.

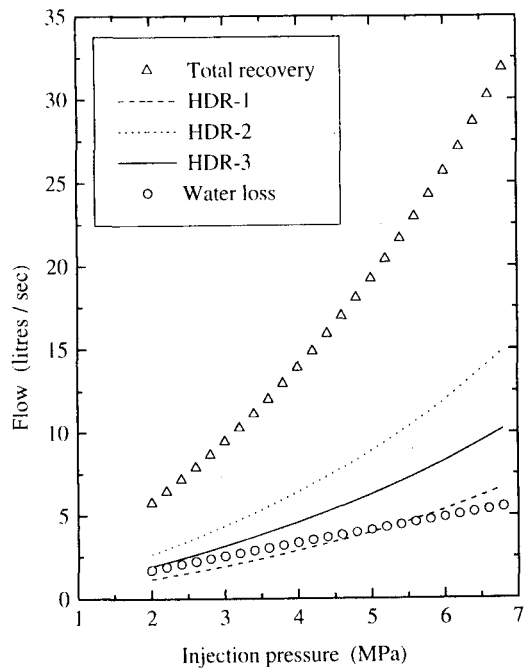


Fig. 5 Model recovery and water loss for the Hijiori 1800m reservoir circulated from SKG-2 to HDR-1, HDR-2 and HDR-3 at different injection pressures

During this test, pairs of production wells were shut in and the injection pressure and remaining recovery flow rate allowed to rise. Only the test with HDR-2 under production appeared to reach a near steady state flow (up 40%) with constant production well-head pressure. The circulation model with HDR-2 alone producing gives a 10% increase in recovery from that well. It is likely that the remaining 30% increase in recovery actually obtained comes from flow to HDR-2 in paths previously directed towards HDR-1 and HDR-3.

## DISCUSSION

The results obtained for Hijiori appear reasonable and utilize the same values for flow path tortuosity and the ratio of total fracture area to reservoir fracture area as was employed for Rosemanowes.

The remaining major uncertainty is the appropriate form of the functional relationship between well separation and total reservoir fracture area. For Rosemanowes we know that a well separation ( $S$ ) of 188m leads to a total fracture area resolvably involved in heat transfer ( $A$ ) of about  $288,000\text{m}^2$ . For Hijiori the individual well production results reported above were obtained with the total fracture areas and separations in Table 3, using the positions of the major flow exits / entries to define  $S$ :

Table 3 Well separation / area values used for the modeling hydraulic performance at Hijiori.

Well pair	S (m)	A ( $\text{m}^2$ )
SKG-2 to HDR-1	43	10000
SKG-2 to HDR-2	52	20000
SKG-2 to HDR-3	86	90000

Figure 5 shows the apparently linear relationship between the well separation and the successful model reservoir fracture areas for Rosemanowes and Hijiori.

However, useful heat extraction capacity will depend on the flux density distribution in the few best flow paths and not just on the total area. For example the SKG-2 to HDR-3 heat extraction during Exp. 9102 was modeled by Tenma et al. (1994) with a heat transfer area of less than  $10000\text{m}^2$ . This is not necessarily inconsistent with the model presented here in which 50% of the flow is frequently associated with 10% of the total area (this is because the model has to generate many "poor" flow paths to find the good ones).

The circulation model used here, whilst capable of generating a good match when the total fracture area is known, is clearly as yet deficient and improved methods are being sought.

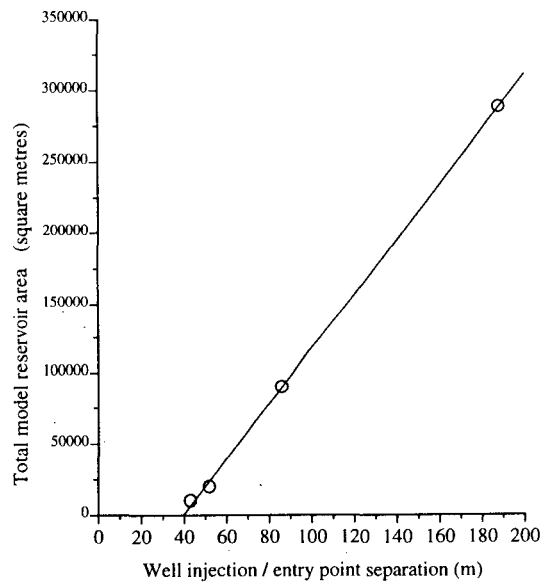


Fig. 6 Tentative relationship between total model reservoir area ( $A$ ) and well separation ( $S$ );  $A = 1940.S - 77000$

Implicit within the stimulation model is the identification of AE with some small fraction of the total fracture shear taking place. The predicted shear movement causes dilation, creating void space equal to the volume of

injected fluid minus the calculated leak off. From this it follows that AE density, if simply related to total shear displacement / area product, is necessarily a good measure of the fluid flow as well as pressure distribution. Were this argument to fail, and aseismic leakoff along "invisible" yet highly permeable features was important, then the predicted and observed RFR's would fail to agree.

## CONCLUSIONS

Since the fracture networks at most HDR research sites in crystalline basement appear to be well connected, it should be possible to make simple numerical models which avoid the complexity and CPU demands associated with an explicit representation of 3-D fracture systems. The models used here are a first step in this direction.

The rock mass descriptive properties which seem to most strongly affect the outcome of HDR stimulation and circulation are identified together with simple methods for their quantification. The small range of fractal dimension exhibited by natural fracture systems greatly reduces the uncertainty at a point where direct underground observations are lacking.

A simple model of shear and shear dilation of single circular fractures is developed as the basis for the description of rock mass stimulation in terms of a rock to fluid ratio (RFR) and the set of apertures of the fractures that result. Good matches to field data for experiments at Rosemanowes, UK and Hijiori, Japan are found.

AE recorded during stimulation are likely to be good predictors of fluid flow paths as well as pressure transmission due to the necessity of significant fluid input to fill the associated shear dilation void space.

Circulation is described by an "in-series" connection of fractures between injection and recovery wells, but a method for adequately predicting the total area of fracture connecting two wells is required. Reasonable descriptions of flow / area partitioning and injectivity curves are easily made, but further developments of this aspect of the model will be made.

Water loss from the margins of the high permeability stimulated volume is calculated using fracture compliance to generate a pressure dependent permeability. Significant water loss by shear dilation during seismogenic circulation is also identified and quantified.

Three important operational lessons emerge. Firstly, stimulation of too large a volume of rock will result in high marginal water losses without useful increase in heat extraction capability. Secondly, increase in the stimulated volume by seismogenic circulation progressively increases marginal water losses without improving inter-well impedance and should be avoided. Thirdly, a good basis exists for associating AE clouds with fluid flow. This enables the use of AE for well targeting with greater confidence.

## ACKNOWLEDGMENTS

J. Willis-Richards acknowledges with gratitude Prof. H. Takahashi of the Research Institute for Fracture Technology, Tohoku University and Prof. K. Nakatsuka of the Dept. of Resources Engineering, Tohoku University for funding his studies in Japan in 1994/5 whilst on sabbatical leave from CSM Associates Ltd., Penryn, Cornwall, U.K.

The work reported in this paper has been possible only as the result of collaboration between the staff of many different organizations sponsored by both the Ministry of Education (Monbusho) and by the Ministry of International Trade and Industry (MITI).

## REFERENCES

- Brown D.W. (1994) How to achieve a four fold productivity increase at Fenton Hill. *Geothermal Resources Council Transactions*, Vol. 18, p 405-408, October 1994.
- Cornet F.H. and Burlet D. (1992) Stress Field Determinations in France by Hydraulic Tests in Boreholes. *Journal of Geophysical Research*, Vol. 97 (B8), p 11,829-11,849, July 1992.
- Clauser C. (1992) Permeability of crystalline rocks. *EOS*, Vol. 73(21), p 233 et seq.
- CSM Associates (1992) Review of HDR Projects. Authors: A.J. Jupe, J. Willis-Richards and J.D. Nichols. Report prepared for AEA Technology, IR03/06, unpublished. 1992.
- Eshelby J.D. (1957) The determination of the elastic field of an ellipsoidal inclusion, and related problems. *Proc. of the Royal Soc. of London, series A*, 241, p 376 et seq.
- Main I.G., Meredith P.G., Sammonds P.R. and Jones C. (1990) Influence of fractal flaw distributions on rock deformation in the brittle field. *Deformation Mechanisms, Rheology and Tectonics, Geological Society Special Publication*, 54, p 81-96, 1990.
- Matsunaga, I. Hiwaki N., Echigoya H. and Okubo S. (1990) Recent progress in Hot Dry Rock project at Hijiori, Japan. *Proceedings of the 12th New Zealand geothermal workshop*, 1990.
- NEDO (1987-1992) Financial Year Summary Reports of Hot Dry Rock Geothermal Power Project in Japan. Geothermal Energy Department, New Energy and Industrial Technology Development Organization, Tokyo.
- Nicol D.A.C. and Robinson B.A. (1990) Modeling the heat extraction from Rosemanowes HDR reservoir. *Geothermics*, Vol. 19(3), p 247-257, 1990.
- Pine R.J., Jupe A.J. and Tunbridge L. (1990) An evaluation of in situ stress measurements affecting different volumes of rock in the Carnmenellis granite. *International Society for Rock Mechanics Workshop on Scale Effects in Rock Masses*, Loen, Norway, June 1990.
- Richards H.G., Parker R.H., Green A.S.P.G., Jones R.H., Nicholls J.D.M., Nicol D.A.C., Randall M.M., Richards S., Stewart R.C. and Willis-Richards J. (1994) The performance and characteristics of the experimental Hot Dry Rock geothermal reservoir at Rosemanowes, Cornwall (1985-1988). *Geothermics*, Vol. 23(2), p 73-109, 1994.
- Watanabe K. and Takahashi H. (1995) Fractal geometry characterization of geothermal reservoir fracture network. *Journal of Geophysical Research*, 1995 (in press).
- Willis-Richards J. (1995) Assessment of HDR reservoir stimulation and performance using simple stochastic models. *Geothermics*, 1995 (submitted).
- Zoback M.L. (1992) First- and second-order patterns of stress in the lithosphere: The world stress map project. *Journal of Geophysical Research*, Vol. 97(B2), p 11,703-11,728, 1992.